XLI CILAMCE
XLI Ibero-Latin American Congress on Computational Methods in Engineering
16-19 November, 2020 FOZ DO IGUAÇU PARANÁ – BRAZIL

Discrete Model Identification of a wind turbine: a case study of Nordtank NTK 330F

Gustavo A. Silveira de Souza[1], Edgar C. Furtado[1], Leandro J. E. Campos[1], Cristiane M. F. Quintão[2]

[1]*Dept. of Telecommunication and Mechatronic Engineering, Federal University of São João del Rei*
Campus Alto Paraopeba, Ouro Branco, Minas Gerais, Brazil
gustagus14@gmail.com, edgar@ufsj.edu.br, leandro.campos@ufsj.edu.br
[2]*Department of Chemical Engineering, Federal University of São João del Rei*
Campus Alto Paraopeba, Ouro Branco, Minas Gerais, Brazil
finzi@ufsj.edu.br

Abstract. The renewable energies are in constant evolution for the sake of the necessity of finding alternatives to fossil fuels derived energy. One of these alternatives are the wind farms, offshore and/or onshore, that provides electricity through the wind force. The horizontal axis turbines are commonly seen on this farms, usually with 3 blades, because of its cost-benefit. However, even though there are equations well defined regarding the behavior of this machines, some environmental variables (such as terrain, height and wind wakes) can add a nonlinear and random factor to the energy conversion. Thereby, the use of system identification shows itself useful to forecast the behavior of this system. In this work, a database from Nørrekær Wind Farm, located on Denmark, is exploited by identification techniques, in order to estimate nonlinear auto-regressive with exogenous inputs (NARX) and auto-regressive with exogenous Inputs (ARX) models. To calculate them properly, three methods will be used and compared: Classical Gram-Schmidt (CGS), Modified Gram-Schmidt (MGS) and Householder-based QR-Decomposition with Column Pivoting. All the methods provided results closer to real data, although MGS and HT models were slightly more accurate.

Keywords: Renewable energy, system identification, wind farms.

1 Introduction

1.1 Context

The technology evolution and growth provide to society on the last decades an abundance of data coming from multiples interactions between humans and machines, like computers, GPS devices, cellphones and medical devices (The World Economic Forum)[1]. This makes any kind of data, nowadays, an extremely valuable information, since its possible to store and large amounts of historical data from any kind of system. In addition, associating the available data with computing intelligence, useful information can emerge, regarding a system and its behavior.

One example of how to use the data is System identification, which, according to Aguirre[2] studies the proceedings that allow to build mathematical models from observed data and signals. This models can predict the system behavior or output, like the power generated by a Wind Turbine .

The Wind Turbines generates electrical energy from wind kinetic energy. This wind conversion is a clean energy generation system, and using it are strictly aligned with sustainable development aimed by United Nations, since the publication of the Brundtland Report [3], in 1987. Moreover, by 2050, the demand for energy could double or even triple, according to Nelson [4], what highlights the search and implementation of new efficient generation systems.

1.2 Objectives

This work aims to compare models generated by three Identification System Techniques: Classical Gram-Schmidt (CGS), Modified Gram-Schmidt (MGS) and Househoulder-based QR-Decomposition with Column Pivoting (HT). This comparison are made using Statistical Validation Indexes, evaluating the quality of each prediction and how accurate the models are.

1.3 Work description

This work intends shows and study of how Identification methods can predict accurately wind turbine behavior, and can be applied to simulate energy generation before it actually happens, given the wind speed series on a place. The models built use a real database obtained with *winddata.com* that contains wind speed and power generation from a Norwegian Wind Farm, called Nørrekær. Moreover, this work shows statistical measurements comparison between validation indexes in order to analyze the quality of the predictions made.

This study can be applied on many other wind turbines. This means that, after defining properly the model of the turbine analyzed, it is possible to predict the power generated by this turbine, using new wind speed databases, knowing the error margin of the prediction. This information can be useful, for example, to analyze viable conditions for building new Wind Farms.

2 Methodology

2.1 The Studied Turbine

The reference used in this work was the turbine Nordtank NTK330F. This turbine has a composite rotor (GPFR – Glass Fiber reinforced plastic), manufactured by LM Glasfiber S/A, with 28m diameter. The blades move through a 615.7m^2 area, with a 39 rpm speed rotation and nominal power of 330kW. The generation begins at 4m/s wind speed (Cut in speed) and is turned off by 25m/s (Cut-out speed). The turbine's inductor generator was manufacturer by Siemens/ABB and the nominal operation occurs at 1500 rpm, generating a voltage of 690V by 50Hz frequency (Bauer and Matysik) [5].

2.2 Turbine's General Behavior

A wind turbine woks, essentially, transforming kinetic energy from the wind in electric energy at the generator's output, as said by Hansen [6]. According to Nelson [4], the kinetic energy come from air molecules movement, so the amount of air molecules moving across some area, during some time, determines the power locally. Besides that, Burton, Sharp, Jenkins and Bossanyi [7] said that the modern wind turbines use the lift forces on the blades to move the rotor. These forces exist due to a difference on the airflow pressure that passes by the laminar surface.

Furthermore, the distance from rotation center also has influence on relative speed vector. This happens because, as higher the rotation radius is, higher the linear speed is as well [8]. The Eq. 1 represents the relation between these two measures [9].

$$v = r\omega, \tag{1}$$

which r is the rotation radius and ω the rotational speed.

This is why the blades have a twisted shape, as the angle of attack can be the most optimal, improving the energy conversion as well.

Finally, the yawing mechanism is responsible to keep the blades constantly wind-aligned. An anemometer posted at the top of turbine tower assures the measurement of the wind direction and then an electronic central acts, when necessary, to rotate the rotor and maximize the energy conversion.

2.3 The Database

The database was bought on *winddata.com*. The data used on tests and simulations correspondent to wind speed and power generated measurements on turbine A1, whose space position inside the wind farm is shown on Fig. 1.

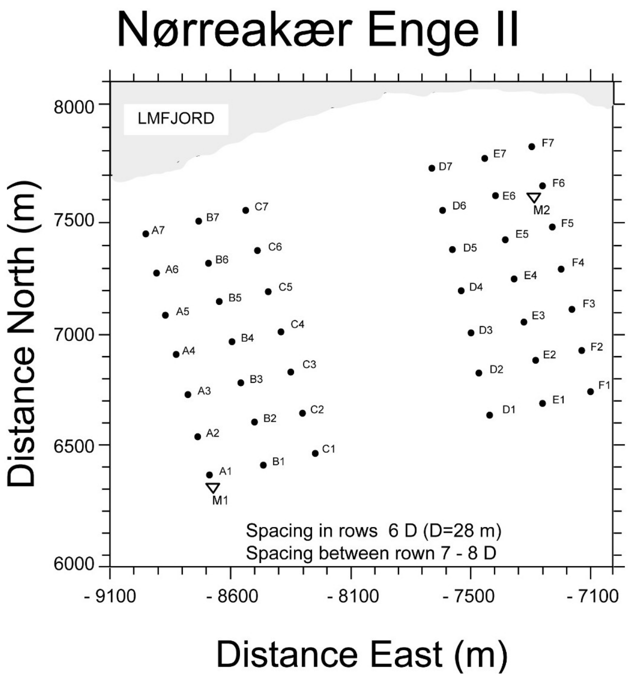

Figure 1. Nørrekær layout. The area covered is 2,1×2,1 km. From [10].

The data used on this study was in the database, according Tab. 1, that presents the fields and meaning respectively.

Table 1. Database fields decription.

Database Field	Field Description
SCAN_ID	An identifier number. As lower the value is, older is the scan.
CHANNEL_ID	Determine what the measurement is about (Wind speed, Power, angle...)
MEAN	Mean data read from sensors.

The time series taken from this database, fit in two periods, divided in: (a) Identification series, which includes wind speed and power generated values between 30/11/1992 19h08min and 04/12/1992 04h53min;(b) Validation series, which includes wind speed values and power generated values between 16/04/1993 00h11min and 19/04/1993 05h51min.

Inside each time series, there is not a significant seasonality interference, although, purposely there were selected time series on two different seasons of the year (winter for identification and spring for validation), evaluating the seasonality impact on generated models.

2.4 Identification Methods

The predictive model development was developed by autoregressive system identification methods, with exogenous inputs. Among the most commons, the ARX and NARX can be highlighted. A more completed approach in terms of autoregressive polynomials models is the NARMAX modeling (Nonlinear Autoregressive Moving Average with eXogenous Inputs), which involves the identification using moving average applied to identification noise, but they will not be into this work. Due to the evaluated system sampling be presented by discrete samples, the model adopted are essentially composed by a difference equation solution [2].

The ARX models (autoregressive with exogenous inputs), can be described as shown on Eq. 2.

$$y(k) = \frac{B(q)}{A(q)}u(k) + \frac{1}{A(q)}v(k), \tag{2}$$

which $v(k)$ represents a noise or uncertainties not modelled, $u(k)$ is the system input and $y(k)$ the output. $A(q)$ and $B(q)$ are polynomials, as:

$$A(q) = 1 + a_1 q^{-1} + \cdots + a_{n_y} q^{-n_y}$$

$$B(q) = b_1 q^{-1} + \cdots + b_{n_u} q^{-n_u}$$

where the q^{-1} is the delay operator, so that $y(k)q^{-1} = y(k-1)$. The ratio $B(q)/A(q)$ is the answer to excitation (or system transfer function) and the ratio $1/A(q)$ is the transfer function that relates noise and output. As the noise is directly on the equation, this belongs to the errors in equation models class (Aguirre) [2]. On the other hand, the NARX models (non-linear autoregressive with exogenous inputs) are discrete in time and explains the output value $y(k)$ as a function of previous outputs and inputs values, as a non-linear equation, as described by Eq. 3.

$$y(k) = f(\Psi(k-1)^T) + e(k), \tag{3}$$

$e(k)$ is the noise or uncertainties not modeled by the invariant time function,f, which non-linearity grade is l. $\Psi(k-1)^T$ contains the regressors output vector, $y(k)$, and regressors inputs vector, $u(k)$, until the instant $(k-1)$(Furtado, Torre and Aguirre) [11], which means,

$$\Psi(k-1)^T = [\Psi_{yu}^T]^T.$$

The great difference between the ARX and NARX models is the non-linearity factor that NARX gives to system identification. As the system studied is non-linear, it hopes to give solutions closer to the real representation. The models in identification systems need some estimators. At the present study, it was used the least squares method for obtaining these estimators. The eq. 4 shows the relation among the observed values ($\overrightarrow{y}$), the regressors matrix (Ψ) and the estimated parameters (θ) (Furtado, Torres and Aguirre) [11].

$$\overrightarrow{y} = [\Psi_{yu}^T]^T[\hat{\theta}_1, \hat{\theta}_2, \ldots, \hat{\theta}_{n_\theta}]^T, \tag{4}$$

From the eq. 4, the only unknown variable is θ. So, to obtain it, it is necessary to solve

$$\overrightarrow{y}(k) = \Psi\overrightarrow{\theta},$$

The matrix manipulation influences directly on models representativeness. To achieve an improved representativeness, it turns out the need for a better parameters estimation. As a result, this study propose evaluate orthonormalization methods to determine this needed better estimation, and consequently, models with improved representativeness.

2.5 Orthonormalization methods for least squares estimation

Classical Gram-Schmidt (CGS): Given a vector space, this method uses the orthonormalization to define a new base. It is a QR factorization method, that transforms a matrix a product typed $A = QR$ (Golub and Van Loan) [12]. It results from consecutive right multiplications by elementary superior triangle matrix, what results in an orthogonal matrix (Trogdon et. al) [13]. Each vector is individually orthogonalized to all previous vectors, what causes a numerical instability and significant stability loss, already on the second iteration, according (Luc, Langou, Rozložník and Van den Eshof) [14]. The Algorithm 1 is an implementation example.

Algorithm 1 Coding example for CGS, where A=QR(Golub and Van Loan) [12]

$R(1,1) = ||A(:,1)||_2$
$Q(:,1) = A(:,1)/R(1,1)$
for $k = 2 : n$ **do**
    $R(1:k-1,k) = Q(1:m,1:k-1)^T A(1:m,k)$
    $Z = A(1:m,k) - Q(1:m,1:k-1)R(1:k-1,k)$
    $R(k,k) = ||z||_2$
    $Q(1:m,k) = z/R(k,k)$

Modified Gram-Schmidt (MGS): This method derives from the previous one. The modification shows itself necessary, due to CGS numerical instability. It is notable their mathematical similarity, differing, essentially, on instructions sequence, and so, the resulting vectors have the same orthonormal structure. The Algorithm 2 shows an example of MGS implementation for the same conditions presented in Algorithm 1.

Algorithm 2 Coding example for MGS (Golub and Van Loan) [12]. Same conditions applied to CGS.

for $k = 1 : n$ **do**
    $R(k,k) = ||A(1:m,k)||_2$
    $Q(1:m,k) = A(1:m,k)/R(k,k)$
    for $j = k+1 : n$ **do**
        $R(j,k) = Q(1:m,k)^T A(1:m,j)$
        $A(1:m,j) = A(1:m,j) - Q(1:m,k)R(k,j)$

Householder-based QR-decomposition with Column Pivoting (HT): This method is used primarily in least square problems classified as rank-deficient (Luc, Langou, Rozložník and Van den Eshof) [14]. Against the decomposition presented on Gram-Schmidt methods, this decomposition is the result from a Ψ left multiplication by a sequence of orthogonal matrix, to reach, at the end, a triangular matrix (Golub and Van Loan) [12]. The Algorithm 3 shows an example of this implementation.

Algorithm 3 Coding example for HT(Golub and Van Loan) [12]

for $(j = 1 : n)$ **do**
    $c(j) = A(1:m,j)^T A(1:m,j)$
$r = 0$
$\tau = max\{c(1), ..., c(n)\}$
while $r > 0$ and $r < n$ **do**
    $r = r + 1$
    Find smallest k with $r \leq k \leq n$ so $c(k) = r$
    $piv(r)$
    $A(1:m,r) \leftrightarrow A(1:m,k)$
    $c(r) \leftrightarrow c(k)$
    $[\nu, \beta] = house(A(r:m,r))$
    $A(r:m,r:n) = (I_{m-r+1} - \beta\nu\nu^T)(A:r:m,r:n)$
    $A(r+1:m,r) = \nu(2:m-r+1)$
    for $i = r+1 : n$ **do**
        $c(i) = c(i) - A(r,i)^2$
    $\tau = max\{c(r+1), ..., c(n)\}$

2.6 Validation indexes

In order to properly compare the results provided by the methods CGS, MGS and HT, there were used statistical validation indexes. They are present as following with their concepts and equations, as presented by Furtado, Silva and Santos [15].

Root mean square error (RMSE). This is one of the most used indexes to measure prediction errors. High RMSE values indicates high prediction errors in model (Heringer de Miranda) [16]. The disadvantage of this method occurs in prediction with large errors, large variance and outlier predictions (Kyriakidis) [17]. It is calculated by eq. 5 where $\hat{y}$ represents the estimated data and y the real data, from validation series.

$$RMSE = \left[\frac{1}{N}\sum_{k=1}^{N}(\hat{y}(k) - y(k))^2\right]^{\frac{1}{2}}, \tag{5}$$

Mean Average percentage Error (MAPE). This index express the error as a real percentage of the real value, which means, smaller its value, higher the model assertiveness (Heringer de Miranda) [16]. A safeguard for this index is its sensibility to null values, as can be saw in eq. 6.

$$MAPE = \frac{1}{N}\sum_{k=1}^{N}\left|\frac{\hat{y}(k) - y(k)}{y(k)}\right|, \tag{6}$$

Theil's U2 (U2). This is a quality prediction index (Furtado, Silva and Santos) [15]. The closer it is from zero, better is the prediction's quality. Despite its similarity with RMSE, this index is different due variance normalization of the real series, as shown on eq. 7, where $\overline{y}$ is the mean of the k samples contained on validation series.

$$U2 = \left[\frac{\sum_{k=1}^{N}(\hat{y}(k) - y(k))^2}{\sum_{k=1}^{N}(\overline{y}(k) - y(k))^2}\right]^{\frac{1}{2}}, \tag{7}$$

Geometric mean relative absolute error (GMRAE). According to Hyndman and Koehler [18], this index has great performance when used to modeling a set of time series. In addition, it compares the absolute error of a given predictive method with a random walk prediction (Armstrong and Collopy) [19]. This index is calculated by eq. 8.

$$GMRAE = \left[\prod_{k=1}^{N}\left|\frac{\hat{y}(k) - y(k)}{\overline{y}(k) - y(k)}\right|\right]^{\frac{1}{N}}. \tag{8}$$

Percent better (PER). It is a percentage index, which implies no unit measure. According to Hyndman and Koehler [18], this index is highly used to compare methods, defining the prediction percentage of a given method that is more precise than random walk. The calculus is defined by eq. 9.

$$PER = \frac{1}{N}\sum_{k=1}^{N} j(k) \times 100, \tag{9}$$

where,

$$j(k) = \begin{cases} 1, & \text{if } |\hat{y}(k) - y(k)| < |\overline{y}(k) - y(k)| \\ 0, & \text{otherwise} \end{cases}$$

3 Results and discussion

Figure 2 exhibits the modulated input data from the identification time series, which is the wind speed measurements, according to their respective date and time. It also shows the output data – or power registered.

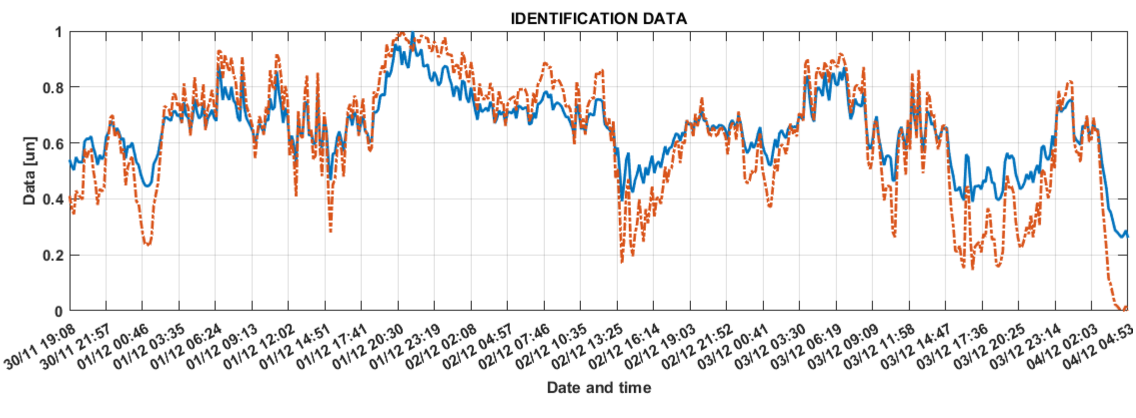

Figure 2. Identification data.

Thereby, there were generated the results for each method analyzed (CGS, MGS and HT), whose values were graphically represented, along with validation data, objecting a visual comparison between the results reached.Figure 3 shows the results obtained. The dotted line shows the values provided by each method.

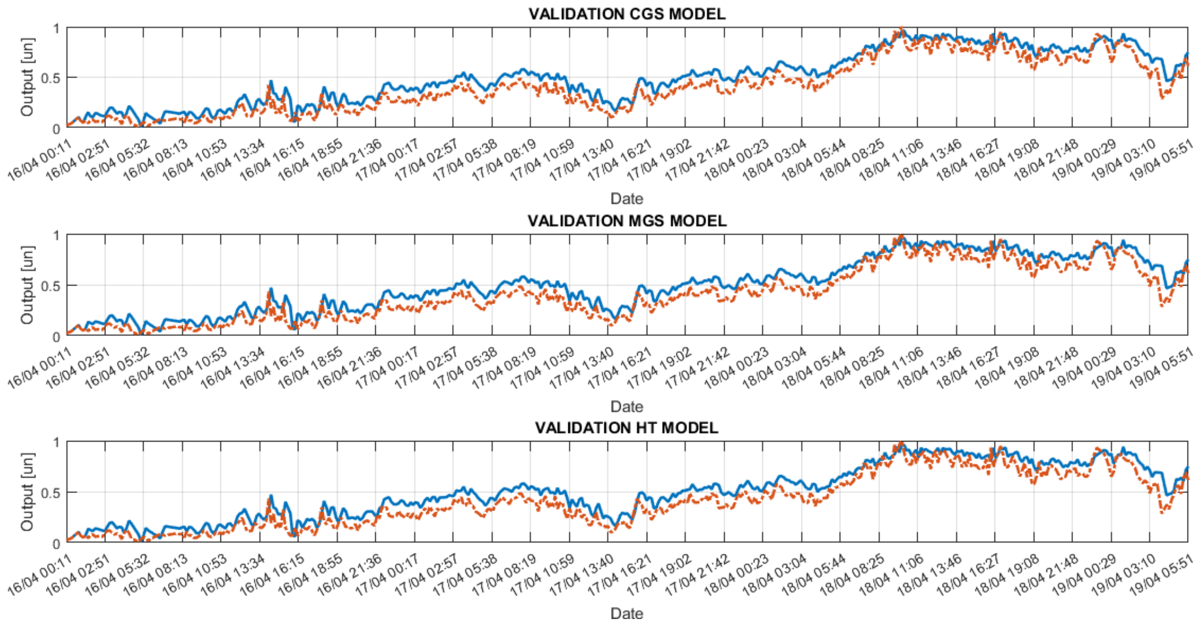

Figure 3. Answer given by CGS, MGS and HT.

For the three methods analyzed, the results were visually satisfactory and the generated model could follow the turbine power generation. Therefore, the validation indexes analysis is necessary to have a more detailed conclusion. The values obtained on the indexes calculus present an overview of which estimation method can be the more properly used for the present system identification. Table 2 provides the values for the five indexes used on validation, associated to the results previously shown. Each column represents a method and each row, an index.

Table 2. Validation indexes evaluation by model.

INDEX	CGS	MGS	HT
RMSE	0.07867	0.07790	0.07790
MAPE	0.19324	0.18081	0.18081
U2	0.36353	0.35997	0.35997
GMRAE	0.40974	0.37641	0.37641
PER	77.8689	79.7137	79.7131

4 Conclusion

The values obtained on Validation Indexes shows that the methods MGS and HT provide results mathematically equals (the differences between the values were roughly 10^{-14}, so it is not possible to determine which one is the best among them. In addition, the CGS indexes could not provide a more accurate result, and, consequently, it has a minor quality of prediction.

Therefore, after comparing the tested methods and validate them by the indexes RMSE, MAPE, U2, GMRAE and PER, it is reasonable to conclude that they are efficient to modeling the system proposed in the time analyzed, which is five days in a sequence.

Authorship statement. The authors hereby confirm that they are the sole liable persons responsible for the authorship of this work, and that all material that has been herein included as part of the present paper is either the property (and authorship) of the authors, or has the permission of the owners to be included here.

References

[1] The World Economic Forum, 2012. Big data, big impact: New possibilities for international development. Technical report.
[2] Aguirre, L. A., 2007. Introdução à identificação de sistemas. *Editora UFMG*, vol. 2.
[3] United Nations, 1987. Report of the world commission on environment and development: Our common future. Technical report.
[4] Nelson, V., 2013. *Wind energy: renewable energy and the environment*. CRC press.
[5] Wind Turbine Models, 2020. *Nordtank NTK 330*. `https://en.wind-turbine-models.com/turbines/1356-nordtank-ntk-330`.
[6] Hansen, M. O., 2015. *Aerodynamics of wind turbines*. Routledge.
[7] Burton, T., Sharpe, D., Jenkins, N., & Bossanyi, E., 2001. *Wind energy handbook*, volume 2. Wiley Online Library.
[8] Channel, L. E., 2020. How do Wind Turbines Work? `https://www.youtube.com/watch?v=mpbWQbkl8_g`.
[9] Young, H. D. & Freedman, R. A., 2008. Física i: mecânica. *Young e Freedman.[Colaborador A. Lewis Ford]. Tradução de Sonia Midori Yamamoto. Revisão técnica de Adir Moysés Luiz*, vol. 12.
[10] Hojstrup, J., Courtney, M., Christensen, C., & Sanderhoff, P., 1993. Full Scale Mesurements in Wind-Turbine Arrays: Nørrekær Enge ii. CEC/JOULE. `http://130.226.56.150/extra/web_docs/norre/norrekaer_windfarm.pdf`.
[11] C. Furtado, E., A B Torres, L., & Aguirre, L. A., 2006. Imposição do ponto de bifurcação por duplicação de períodos em modelos nar polinomiais. *CBA*.
[12] Golub, G. H. & Van Loan, C. F., 2013. *Matrix Computations*. Baltimore: The Johns Hopkins University Press, 4th edition.
[13] Trogdon, T., 2016. The modified gram-schmidt procedure. `https://www.math.uci.edu/~ttrogdon/105A/html/Lecture23.html`.
[14] Luc, G., Langou, J., Rozložník, M., & Van Den Eshof, J., 2005. Rounding error analysis of the classical gram-schmidt orthogonalization process. *Numerische Mathematik*, vol. 101.
[15] Furtado, E. C., Silva, V. C., & Santos, D., 201? Implicação da escolha de diferentes medidas de erro na estrutura de modelos narma para previsão de demanda elétrica. *UFMG*.
[16] Heringer de Miranda, I. P., 2014. Comparação de diferentes métodos de previsão em séries temporais com valores discrepantes. *Undergraduate thesis*.
[17] Kyriakidis, I., 2015. New statistical indices for evaluating model forecasting performance.
[18] Hyndman, R. J. & Koehler, A. B., 2006. Another look at measures of forecast accuracy. *International journal of forecasting*, vol. 22, n. 4, pp. 679–688.
[19] Armstrong, J. S. & Collopy, F., 1992. Error measures for generalizing about forecasting methods. *International journal of forecasting*, vol. 8, n. 1, pp. 69–80.